Single-File Diffusion of Confined Water Inside SWNTs: An NMR Study

Anindya Das,[†] Sundaresan Jayanthi,[†,‡] Handiganadu Srinivasa Murthy Vinay Deepak,[§] Krishna Venkatachala Ramanathan,[‡] Anil Kumar,[†,‡] Chandan Dasgupta,[†] and Ajay K. Sood[†,*]

[†]Department of Physics, Indian Institute of Science, Bangalore 560012, India, [‡]NMR Research Centre, Indian Institute of Science, Bangalore 560012, India, and [§]Physics Department, Jain University, Bangalore 560004, India

ABSTRACT We report a nuclear magnetic resonance (NMR) study of confined water inside ~1.4 nm diameter single-walled carbon nanotubes (SWNTs). We show that the confined water does not freeze even up to 223 K. A pulse field gradient (PFG) NMR method is used to determine the mean squared displacement (MSD) of the water molecules inside the nanotubes at temperatures below 273 K, where the bulk water outside the nanotubes freezes and hence does not contribute to the proton NMR signal. We show that the mean squared displacement varies as the square root of time, predicted for single-file diffusion in a one-dimensional channel. We propose a qualitative understanding of our results based on available molecular dynamics simulations.

KEYWORDS: carbon nanotubes · water · confinement · single-file diffusion · NMR

Confinement of water molecules at the nanoscale[1] has attracted a lot of attention in recent years from the fundamental physics point of view as well as its relevance to biology, geology, and material science. The physical properties of confined water and diffusion in reduced dimensionality exhibit a number of peculiarities in comparison with the bulk water. Single-walled carbon nanotube (SWNT) is an excellent material to provide a nanoscale geometry to confine the water molecules that have a weak interaction with the carbon nanotube.[2] In recent years, molecular dynamics simulation (MD),[3−7] grand canonical Monte Carlo simulation,[8,9] X-ray diffraction,[10] neutron diffraction,[11] inelastic neutron scattering (INS),[11] and nuclear magnetic resonance (NMR) techniques[12−15] have been used to study the water confined inside the SWNTs. In these studies, it has been shown that the water molecules enter inside the SWNTs, and their physical properties are drastically modified due to disruption of the hydrogen bond network. The average number of hydrogen bonds is reduced within the nanotube relative to four in bulk water, resulting in lowering of the freezing (melting) transition temperature of the confined water.[6,7]

Molecular dynamics simulations,[11] neutron scattering experiments,[11] and grand canonical Monte Carlo simulations[8] show that, inside a nanotube of diameter ~1.4 nm, water molecules are organized in a "shell"-like structure near the wall and a "chain"-like structure near the center of the SWNT. The chain-like water molecules show liquid-like behavior even at temperature as low as ~50 K, which is far below the nominal freezing point of bulk water (273 K). However, the dynamics of shell-like water molecules is similar to that of ice. The high mobility of chain-like water molecules is believed to arise due to the hydrophobic nature of the inner region.[11]

Molecular diffusion in a unidimensional channel is very different from that of isotropic diffusion in the bulk system. The restricted geometry makes mutual passage between the molecules forbidden, and as a result, the sequence of molecules remains the same over time. Time dependence of mean squared displacement (MSD) with time (t) characterizes the nature of diffusivity: MSD in ordinary diffusion varies linearly with time, whereas it increases as the square root of time in unidimensional channels.[16−18] The latter is known as single-file diffusion (SFD).[19−21] Diffusion in restricted geometry is of interest in understanding the diffusion in nanoporous zeolites,[22] ion transport in biological membranes,[19,23−26] catalysis,[27] and drug release, *etc.* It has been shown experimentally that diffusion of CH_4 gas molecules inside zeolite $AlPO_4$-5 is SFD by measuring the time dependence of the MSD using the pulsed field gradient (PFG) NMR technique.[22,28−30] So far, molecular dynamics simulation has been employed to understand the diffusive nature of confined

*Address correspondence to asood@physics.iisc.ernet.in.

Received for review November 4, 2009 and accepted February 23, 2010.

Published online March 4, 2010.
10.1021/nn901554h

water inside the SWNT.[31,32] There are no experimental results of the MSD of confined water inside the SWNT.

Nuclear magnetic resonance spectroscopy is a unique technique to study the confined water inside the SWNT. This is because the NMR transverse (spin−spin) relaxation time, T_2, of a proton in water is much larger (100 ms to a few seconds) than that of solid ice (~6 μs). This ensures that the NMR signal below 273 K (the freezing temperature of bulk water) arises essentially from the nonfrozen confined water inside the SWNT. Let us briefly summarize the existing NMR results on confined water inside SWNTs. Ghosh *et al.*[12] showed that the ^{1}H NMR signal of confined water inside SWNTs (diameter ~1.4 nm) has two components: broad L_1 component (line width ~10 kHz) associated with the water molecules at the center of the SWNT, which vanishes below 242 K; and a narrower L_2 component (~4 kHz) associated with water molecules near the wall of the SWNT whose intensity decreases to zero near 212 K. Mao *et al.*[13] have measured the water adsorption isotherms at room temperature inside SWNTs (~1.4 nm) and shown that the capacity of water inside the SWNT is 3 mmol/g, whereas molecular dynamics predicts that it should be 16 mmol/g. The ^{1}H NMR signal has a single peak line width of 5 kHz. Sekhaneh *et al.*[14] assigned the chemical shift of outside water compared to the inside water in a ~1 nm SWNT using ^{1}H MAS (magic-angle spinning) NMR spectroscopy. The proton NMR line width of confined water is ~0.8−1 kHz. Matsuda *et al.*[15]have investigated ^{2}H and ^{1}H NMR between 100 and 300 K inside ~1.35 nm SWNTs. They have calculated the ^{1}H NMR line width to be ~24 kHz for intramolecular ^{1}H−^{1}H dipole interaction in confined water, whereas the intrinsic ^{1}H NMR line width is ~1−3 kHz due to intermolecular dipolar broadening. However, experimentally, they have observed a single ^{1}H NMR peak at ~5 kHz up to 200 K, and below this temperature, there are two lines, one with narrow line width (~5 kHz) and another one with very broad line width (~50 kHz). They attributed the narrow and broad lines, respectively, to the mobile and immobile water molecules.

All of these studies show that the confined water inside SWNTs has liquid-like behavior far below 273 K. In most of the cases, a motionally narrowed single peak (0.8−5 kHz) is observed for confined water. However, there is no clear experimental evidence whether these NMR signals come from the center of the nanotube (chain-like water) or near the wall (shell-like water). Most importantly, there is no dynamic study to find the diffusive nature of confined water inside SWNTs. In this paper, we report proton nuclear magnetic studies of confined water inside the single-walled carbon nanotube with an average diameter of ~1.4 nm. We divide our results into two sections: (i) static and (ii) dynamic. In the static part, we confirm that the confined water does not freeze up to 223 K, and in the dynamic part, we present MSD of the water molecules moving inside the SWNT, which reveals single-file diffusion. From the narrow line width observed in the static part and the MSD dependence on time as $\sqrt{t}$, we propose that the single peaked narrower ^{1}H NMR signal (~300 Hz) comes from the mobile chain-like water molecules near the center of the SWNT.

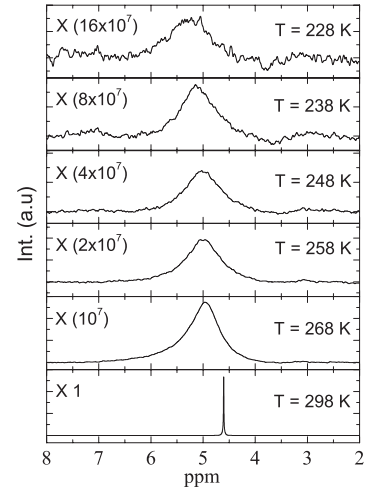

Figure 1. Temperature dependence of the proton NMR spectrum using an AMX-400 NMR spectrometer. The multiplicative intensity scale factors and corresponding temperatures are shown in each panel.

RESULTS AND DISCUSSIONS

Static Part. Figure 1 shows the ^{1}H NMR spectra recorded at different temperatures. The temperatures of the sample (SWNT + H_2O) were lowered slowly from room temperature to ~223 K at an interval of 5 K, and at each temperature, the sample was equilibrated for 30 min. In the heating cycle, we repeated the same procedure and recorded the NMR spectra shown in Figure 1. The intensity scale factors are given at the left side of the spectra normalized by the number of scan (NS = 1) and receiver's gain (RG = 1). At 298 K, a narrow peak (width ~8 Hz) is observed. Because a very small weight fraction (~10^{-3}%) of nanotubes is used in SWNT/H_2O mixtures, the contribution of the confined water (water molecules inside the SWNT) at 298 K will be negligible compared to the bulk water outside the nanotubes. Below the bulk freezing temperature (273 K), the water molecules outside the SWNT freeze, and therefore, the broader peaks (width ~300 Hz) below 273 K in Figure 1 arise from the mobile water molecules confined inside the SWNT. It has been discussed in the introduction that the water molecules do not freeze inside the SWNT due to lower coordination number, and as a result, they are mobile inside the SWNT and contribute to the NMR signal. It can be seen from Figure 1 that the NMR intensity of the confined water is ~10^{-7} times less compared to the bulk water signal. We should note that the NMR spectra of confined water are symmetric with a single peak, and its position is down shifted compared to the bulk water. The NMR

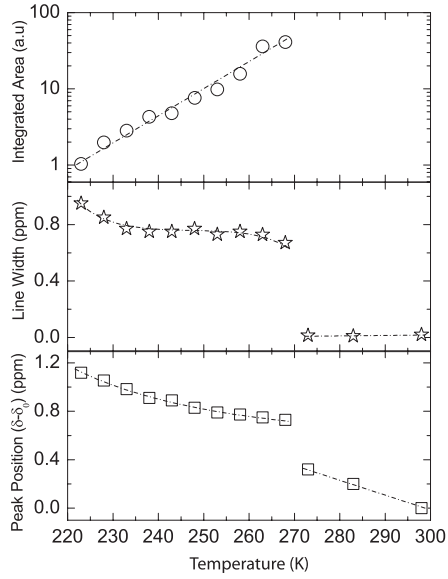

Figure 2. (Top panel) Integrated area normalized by NS = 1 and RG = 1 as a function of temperature. Line width (middle panel) and chemical shift (bottom panel) of the NMR spectra at different temperatures. The dotted lines are drawn as a guide to the eyes. The integrated intensities for free water (above 273 K) are very large and not shown here.

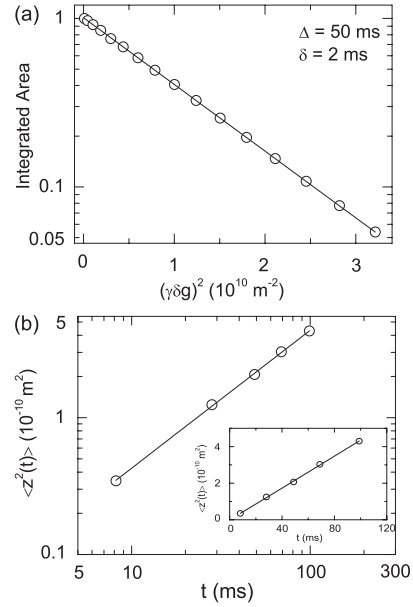

Figure 3. (a) PFG NMR attenuated signal of a SWNT+ H_2O mixture at 298 K using a DRX-500 NMR spectrometer. The integrated area is normalized by the signal at a gradient field strength (*g*) of zero. (b) MSD as a function of observation time (*t*) in log−log scale. Inset shows the same data in linear−linear scale.

spectra are fitted with a single Lorentzian, and in Figure 2, we show their area, line width, and peak position as a function of temperature. As temperaure is lowered, the integrated area decreases, and below 223 K, it is barely observable due to a poor signal-to-noise ratio. To explain the intensity decrease with lowering of temperature, we follow ref 3, where they have shown, using MD simulation, that there are two radial density distributions inside the SWNT: one near the center of the nanotube and another one near the wall. With decreasing temperature, the water molecules move from the center to the wall, and as a result, the fraction of the water molecules at the center of the nanotube decreases. It can be seen from the middle panel of Figure 2 that the line width of bulk water is ~0.02 ppm (0.02 × 400 = 8 Hz), whereas the line width of the confined water is ~250 Hz and it remains constant up to 240 K and then increases up to 400 Hz at 223 K. This line width (0.25−0.4 kHz) is very close to the calculated intrinsic line width (1−3 kHz) of the ^{1}H NMR of confined water.[15] Therefore, almost constant narrow line width (~300 Hz) with decreasing temperature is likely to arise from the mobile part of the confined water with translational and quasi-rotational motion, implying that there is no signature of freezing even up to 220 K. This is consistent with the neutron scattering results of ref 11, where the freezing is suppressed up to 50 K. In the present experiment, the line width (~400 Hz) is very narrow as compared to the one in earlier experiments (~10 kHz).[12] The only difference is we use a very small amount of nanotubes (0.006% weight fraction, *i.e.*, 100 μg of high purity SWNT in 1.6 mL of double distilled water) compared to our earlier experiments[12] (2.5 mg of SWNT completely soaked in double distilled water). We believe that the magnetic shielding effect is one of the major factors contributing to the NMR line width of the confined water inside the carbon nanotube. As seen in the bottom panel of Figure 2, the chemical shift of the bulk water increases with decreasing temperature because of density change. The chemical shift of the confined water also increases with the decreasing temperature. A sudden jump in position of the chemical shift of the confined water compared to the bulk water at 273 K may arise due to anisotropic magnetic susceptibility of the SWNT and disrupted hydrogen bond network of the confined water.

Dynamic Part. In the dynamic part, we have used the pulsed field gradient (PFG) NMR method (see the Experimental Section for the details) to determine the diffusion of water molecules. We recorded the PFG NMR signal for 16 different values of gradient magnetic field strength (*g*), and then we fit each spectrum with a single Lorentzian. Figure 3a shows the decrease of attenuated PFG NMR signal (normalized integrated area) as a function of the quantity $(\gamma\delta g)^2$ at $T = 298$ K for $\Delta =$ 50 ms, where the diffusive time $t = \Delta - \delta/3$ and δ (the duration of gradient pulse) = 2 ms. The details have been described in the Experimental Section. It can be seen from Figure 3a that in log−linear scale the attenuated signal depends linearly on the square of the gradient field strength. We have fitted the experimental data (open circles in Figure 3a) using the following equation:[33]

$$\frac{I}{I_0} = \exp\left(-\gamma^2 g^2 \delta^2 \frac{\langle Z^2(t)\rangle}{2}\right) \qquad (1)$$

with mean squared displacement ($\langle Z^2(t)\rangle$) as a fitting parameter. The I_0 corresponds to the signal for $g = 0$. Figure 3b shows the MSD ($\langle Z^2(t)\rangle$) in log−log scale for different diffusive times (open circles). The MSD is fitted with the equation

$$\langle Z^2(t)\rangle = 2Dt \qquad (2)$$

where, D, diffusion coefficient of the bulk water is the fitting parameter. The inset of Figure 3b shows the MSD ($\langle Z^2(t)\rangle$) as a function of time in a linear−linear scale, and it can be seen that the mean squared displacement increases linearly with time, as expected for normal diffusion. Thus, at $T = 298$ K, bulk water shows normal diffusive behavior with diffusion coefficient $D = 2.2 \times 10^{-9}$ m^2/s. As mentioned in the static part, because of the very low weight fraction of the SWNT sample, the PFG NMR signal at 298 K comes mainly from outside bulk water.

To find the diffusive nature of confined water inside the SWNT, we slowly cooled the SWNT/H_2O mixture from room temperature to 220 K at an interval of 5 K and waited for 30 min at each temperature. The sample is then slowly heated in 5 K intervals with a wait of 30 min, and the PFG NMR signals are recorded in the heating cycle. The diffusive nature of confined water is determined at two temperatures, 271 and 268 K, because at still lower temperatures PFG NMR signals become too weak to record 16 values of gradient magnetic field strength (g). The inset of Figure 4a confirms that the static ^{1}H NMR spectra of the confined water (broader line) at 271 K and that of the bulk water (narrow line) at 298 K recorded at 500 MHz spectrometer are nearly identical to those recorded using a 400 MHz spectrometer (Figure 1). Figure 4a shows the PFG NMR spectra of the confined water inside the SWNT at $T = 271$ K for several gradient magnetic field strengths (g) for $\Delta = 150$ ms. Each spectrum is fitted with a single Lorentzian, and the normalized integrated areas are shown in Figure 4b as a function of the square of the gradient field strength. It can be seen from Figure 4b that the attenuated NMR signal does not decay linearly in log−linear scale as opposed to the case of the bulk water (Figure 3a). This can be understood by the following argument. The signal attenuation for the confined water in a unidimensional channel can be written as[34,35]

$$\frac{I}{I_0} = \frac{1}{2}\int_{-1}^{1} \exp\left(-\gamma^2 g^2 \delta^2 \frac{\langle Z^2(t)\rangle}{2} x\right) dx \qquad (3)$$

where the integral over the parameter x (cos θ) arises to take into account the random orientation of the nanotubes with respect to the direction of gradient field strength (g). The experimental data (open circles in Figure 4b) are fitted using eq 3 with MSD ($\langle Z^2(t)\rangle$) as a fitting parameter, as shown by the solid line in Figure 4b. Therefore, from the sublinear decay profile of the PFG attenuated signal, we confirm that at 271 K the NMR

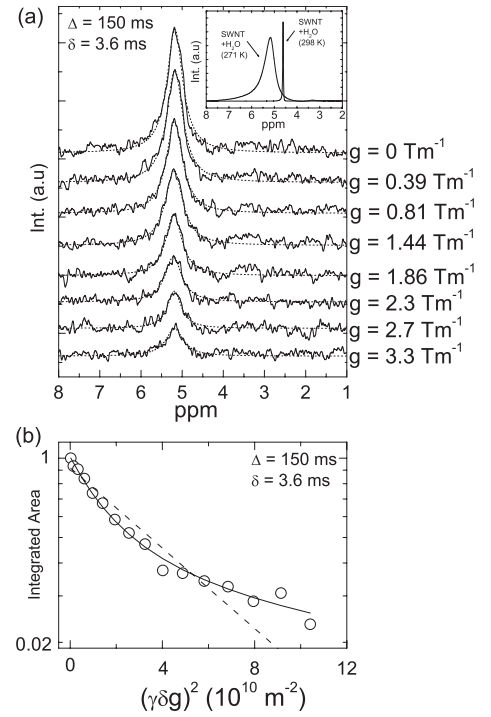

Figure 4. (a) PFG NMR spectra of a SWNT + H_2O mixture at 271 K for different gradient field strength (g). The dotted lines are the fitted Lorentzians. Inset shows the static NMR spectra at 298 and 271 K (×10^7). (b) Attenuated normalized integrated area of the confined water at 271 K as a function of square of gradient field strength (g). The solid line is fitted using eq 3, and the dashed line is fitted using eq 1.

signal comes from the confined water inside the SWNT. Figure 5a shows these sublinear decay profiles of attenuated signal of the confined water for different diffusive times. The solid lines are the fitted curves using eq 3 to get MSD ($\langle Z^2(t)\rangle$), as shown in Figure 5b in log−log scale. The inset in Figure 5b shows the data in linear−linear scale and can be seen that, unlike bulk water, the mean squared displacement of the confined water does not increase linearly with time. We fitted the MSD with the equation

$$\langle Z^2(t)\rangle = 2Ft^{\alpha} \qquad (4)$$

where the best fit is obtained for $\alpha = 0.54 \pm 0.02$ and the mobility $F = 3.26 \times 10^{-10}$ m^2 s$^{-1/2}$, as shown by the solid line in Figure 5b. The same experiment was repeated at 268 K, and Figure 6 shows the attenuated signal of the confined water as a function of square of the gradient field strength for different PFG delay time (Δ). In Figure 7, we have compared the mean squared displacement at three temperatures (298, 271, and 268 K) as a function of observation time (t). The 268 K data are also fitted using eq 4 with $\alpha = 0.53 \pm 0.03$ and $F = 1.03 \times 10^{-10}$ m^2 s$^{-1/2}$. We can see that the MSD depends as the square root of time, and therefore, we conclude that the diffusion of the confined water inside the SWNT is single file in nature.

SFD in a unidimensional channel is only possible if the particles cannot cross each other. In a 1.4 nm tube,

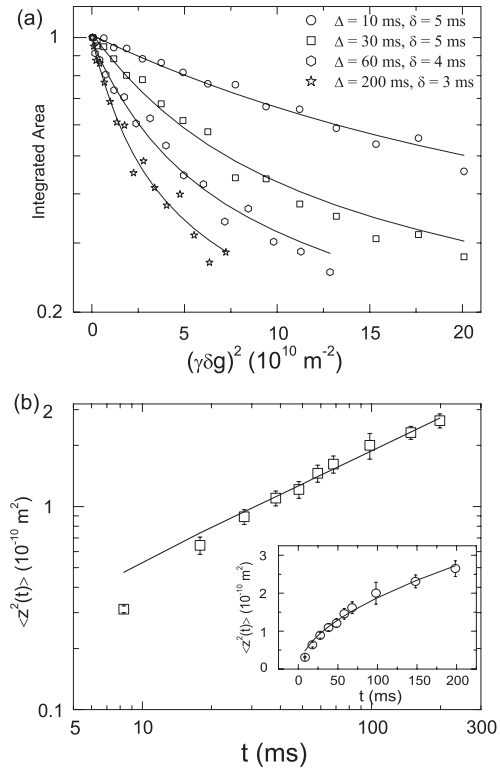

Figure 5. Normalized attenuated PFG NMR data of the confined water at 271 K for different observation time ($t = \Delta - \delta/3$). (b) MSD as a function of observation time (t) in log−log scale. Inset shows MSD in linear−linear scale.

water molecules should be at a distance 0.27 nm from the wall of the nanotube because of the hydrophobic van der Waals gap.[36] Therefore, only 0.86 nm is available for the confined water, which can accommodate about three water molecules in the cross section of the nanotube. Thus, on first sight, SFD may not be expected to be observed in a 1.4 nm diameter tube. Here, we give a plausible explanation for the observation of SFD. As mentioned in the introduction, the confined water molecules inside the 1.4 nm tube make shell- and chain-like structures, as seen in MD simulations.[11] Below 273 K, the molecules in the shell-like structure become immobile along the interior of the nanotube wall in a four-fold coordinated "square-ice" pattern. However, the water molecules in the central chain-like structure with an average coordination number of 1.9 have large translational and rotational motion even up to 50 K. Thus, the narrow (~0.3 kHz) NMR signal seen in our experiments essentially comes from the chain-like central water molecules. The NMR signal from the shell-like water molecules (with an expected line width of about 24 kHz due to $^1H-^1H$ dipole interaction[15]) could not be seen in our experiment due to limited spectral window (~10 kHz). The chain-like central water molecules move in a unidimensional channel where they cannot pass each other and hence exhibit single-file diffusion. The large MSD seen in Figure 7 suggests that the water molecules in the chain are not close-packed. We should mention here that, in our understanding, the narrow line in ref 15 can arise from the central chain-like (mobile) molecules, whereas the broad line below 200 K can be attributed to shell-like (immobile) water molecules. We should also mention that more theoretical work is needed to achieve better understanding of our data. We want to emphasize that our explanation of the single-file diffusion in terms of a model given above (ref 11) is only qualitative and suggestive. We do not claim that the shell-central chain model is the only possibility to understand our results. It could be possible that the observed one-dimensional behaviors may arise from the water clusters inside the SWNT, where the clusters exhibit the single-file diffusions inside SWNTs with larger diameter cavities. We hope this will motivate further simulations to understand the dynamics of confined water inside nanotubes.

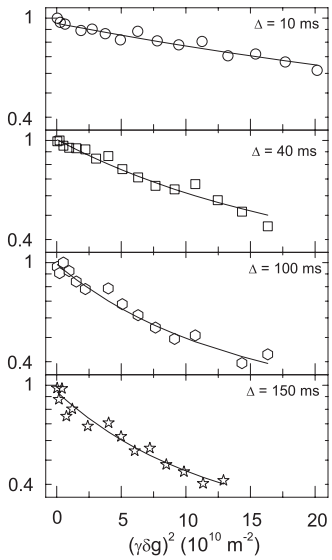

Figure 6. Normalized attenuated PFG NMR data of the confined water at 268 K for different observation time (t).

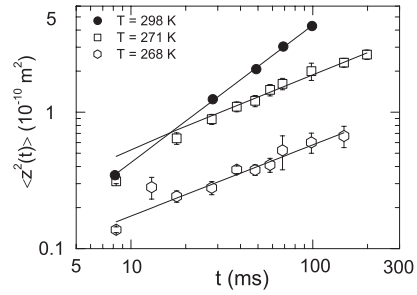

Figure 7. Comparison between the MSD at different temperatures. At 298 K, the solid line is the fitted line using eq 2. At 271 and 268 K, the solid lines are fitted using eq 4, yielding $\alpha = 0.54$ and 0.53, respectively.

Here we should also point out that there are additional surfaces as well as interstitial spaces available in SWNTs, and those can contribute to the NMR signal. However, we rule out these possibilities: single-walled carbon nanotubes (SWNTs) self-assemble into a two-dimensional triangular lattice to form bundles of aligned nanotubes with a nearest intertubular gap of ~0.34 nm. These interstitial gaps in the bundle can be

potential sites for the water molecules. However, molecular dynamics simulations have shown that the water molecules do not enter the hydrophobic van der Waals gaps between the nanotubes in a bundle.[37] This is understandable because first principle calculations show that the water molecules should be at a distance of ~0.27 nm from the surface of the nanotubes.[36] Even though the nanotube surface is corrugated, the structural properties of water at the nanotube−water interface are similar to those seen for water at an idealized graphite surface.[38] The enthalpies of water-immersed singe-walled carbon nanotube horns showed a very weak interaction between the water molecules and the hydrophobic carbon nanotubular structure.[39] Since our earlier NMR experiments[12] on water adsorbed on graphite did not show any measurable suppression of the freezing/melting temperature of water, we rule out the possibility of contributions from adsorbed water on the nanotube surface to the NMR spectra below 273 K. The only difference in the case of the nanotube compared to graphite surface is the presence of a few $COOH^-$ groups at two ends of the nanotubes, where the water molecules can be adsorbed and can contribute to the NMR signal. However, these water molecules can contribute only to the static NMR signal and not to the dynamics, which shows a large mean squared displacement as well as sublinear decay profile of the PFG attenuated signal below 273 K. Thus, we believe that the NMR proton signals in our diffusion experiment come from the confined water inside the nanotube.

In order to substantiate our interpretation of the observed dependence of the MSD on time as evidence for single-file diffusion, it is necessary to establish that the observed behavior is not due to the finite size and size distribution of the nanotubes. Since the nanotubes have finite length, the MSD of a molecule undergoing normal diffusion inside a nanotube is expected to saturate at times on the order of the time that the molecule takes to diffuse over a distance comparable to the length of the nanotube (we assume here that the molecules cannot exit the nanotube through its ends). The MSD in this case would grow linearly with time at short times but would deviate from linear growth at longer times, eventually saturating in the long time limit. For such a dependence of the MSD on time, it is always possible to find a time interval over which the dependence of the MSD on time is reasonably well-described by a power law with an exponent close to 1/2. This effect may be accentuated by the fact that the lengths of all of the nanotubes in the sample are not the same: a distribution of lengths may increase the size of the time interval over which the MSD of normally diffusing molecules, averaged over the distribution of the lengths of the nanotubes in the sample, exhibits a time dependence similar to that expected for single-file diffusion. We have studied the effects of finite size and size distribution on the time dependence of the MSD of molecules undergoing normal diffusion in one dimension in order to examine whether the observed behavior can be explained in terms of these effects.

Our calculations are based on the one-dimensional diffusion equation with reflecting boundary conditions. Let $P(x, t|x_0, 0)$ be the probability of finding the diffusing particle at position x at time $t > 0$, assuming that it is at x_0 at time $t = 0$. This quantity satisfies the diffusion equation

$$\frac{\partial P}{\partial t} = D\frac{\partial^2 P}{\partial x^2} \tag{5}$$

where D is the diffusion constant. The boundary conditions for a particle inside a tube of length L with reflecting boundaries are

$$\frac{\partial P}{\partial x} = 0 \text{ at } x = 0,\ L \text{ for all } t > 0 \tag{6}$$

and the initial condition is $P(x, t|x_0, 0) = \delta(x - x_0)$ at time $t = 0$. It is easy to show that the solution of eq 5 under these conditions is given by

$$P(x, t|x_0, 0) = \frac{1}{L}\sum_{n=-\infty}^{\infty} \cos(k_n x_0)\cos(k_n x)e^{-Dk_n^2 t} \tag{7}$$

where $k_n \equiv n\pi/L$ and n is an integer. Using this solution, it is quite straightforward[32] to calculate the MSD, $\langle\Delta x^2\rangle$, as a function of time t. The result, after averaging over the initial position x_0, is

$$\frac{\langle\Delta x^2\rangle}{L^2} = \frac{1}{6} - \frac{4}{\pi^4}\sum_{m=1}^{\infty}\frac{1}{m^4}[\cos(m\pi) - 1]^2 e^{-Dk_m^2 t} \tag{8}$$

It is clear from the above equation that $\langle\Delta x^2\rangle/L^2$ is a universal function of Dt/L^2 that saturates at 1/6 at long times. A plot of this function in log−log scale is shown in Figure 8 (solid line). The plot (open circles) also shows the results of a simulation of a random walk inside a tube closed at both ends. The numerical results agree very well with the analytic prediction. The plot also shows power laws with exponent 1 (normal diffusion) and 1/2 (single-file diffusion) as straight lines in the

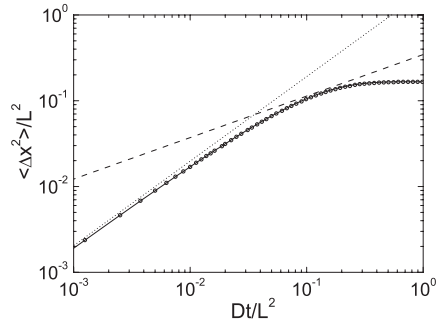

Figure 8. Theoretical calculations using eq 8. The solid line and open circles correspond to the analytical and numerical calculations, respectively. The power laws with exponents of 1 and 1/2 are shown by dotted lines and dashed lines, respectively.

log−log scale. It is clear that the MSD increases linearly with time at very short times, but the effective exponent (slope of the curve in the log−log plot) that describes the time dependence of the MSD decreases with time, becoming zero at long times. This plot also shows that the width of the time interval over which the effective exponent is close to 1/2 is rather small. Quantitatively, the time interval in which the effective exponent changes from 0.55 to 0.45 corresponds to an increase of t by a factor of 1.3. This is much smaller than the width of the interval over which a power law with an exponent close to 1/2 is observed in the experiment: in both plots shown in Figure 7, the time t changes by a factor of about 10. Thus, the observed behavior of the MSD cannot be understood as normal diffusion in a tube of finite length.

To examine the effects of a distribution of tube lengths, we have averaged the result for $\langle \Delta x^2 \rangle$ over several broad distributions of the length L and found that the time dependence of the average MSD is very similar to that of the MSD in a tube of length equal to the average of the distribution used in the calculation. Thus, the conclusion of the analysis described above is not affected by a distribution of the lengths of the nanotubes.

The behavior of the MSD in single-file diffusion in a closed tube is also affected by the finite size of the tube. It is, therefore, important to examine the conditions under which the MSD of single-file diffusion in a closed tube follows a power law in time with an exponent of 1/2. We have studied this question by performing simulations of a simple model[40] of single-file diffusion in tubes of finite length. In this model, a collection of hard-core particles hops on a one-dimensional lattice. At each step of the simulated process, a randomly chosen particle attempts to hop to its nearest neighbor, either to the left or to the right, with equal probability. An attempted hop is accepted if the site to which the particle attempts to hop is empty. This model is known[40] to lead to single-file diffusion at long times if the size of the lattice is sufficiently large. We have simulated this process on lattices of different size, using reflecting boundary conditions at the two ends. An important parameter in this model is the average separation δ between two neighboring particles, defined as $\delta = L/n - 1$, where n is the number of particles and L is the number of lattice sites. We find that the range of time (measured as the number of attempted hops per particle) over which the MSD shows a power-law dependence on time with an exponent close to 1/2 (*i.e.*, behavior characteristic of single-file diffusion) depends on the value of δ/L. For values of δ/L smaller than 0.01, this range of time covers more than a decade. The average spacing between neighboring water molecules in a nanotube is expected to be much smaller than the typical length of a nanotube in the experimentally studied sample. Therefore, our results imply that it is certainly possible to observe a $\sqrt{t}$ time dependence of the MSD for single-file diffusion in finite tubes.

CONCLUSION

In conclusion, we have for the first time experimentally measured the single-file diffusion of the confined water molecules inside SWNTs. We have proposed that, at temperatures below 273 K, ^{1}H NMR signal arises from the mobile water molecules inside the nanotubes. More NMR experiments are desirable on different liquids in carbon nanotubes of different diameters to understand the dynamics of liquids at the nanoscale.

EXPERIMENTAL SECTION

NMR measurements were performed using Bruker 400 MHz AMX-400 and 500 MHz DRX-500 FT-NMR spectrometers. For static measurements performed using the 400 MHz spectrometer, the ^{1}H NMR spectra were acquired with a $\pi/2$ pulse of length of 4 μs. The total number of scans (NS) and receiver's gain (RG) varies in different temperature runs to optimize the signal-to-noise ratio. Above the freezing temperature of bulk water (273 K), NS = 32 and RG = 1, whereas below 273 K, NS = 512 and RG = 8192 were used to obtain the best quality NMR signals. The temperature variation was achieved using a Bruker temperature controller with a temperature stability better than ±0.1 K.

SWNT bundles were prepared by the arc discharge method followed by a purification process, involving acid washing and high-temperature hydrogen treatment.[41] The nanotubes are characterized by the thermogravimetric analysis, transmission electron microscopy,[41] Raman spectroscopy,[41] and near-infrared spectroscopy.[41] The average diameter of the nanotubes was about 1.4 nm, with the length being a few micrometers (5−15 μm). One hundred micrograms of the SWNT sample was suspended in 1.6 mL of double distilled water. The solution was sonicated for 1 h at a power level of 3 W to get the homogeneous dispersion of nanotubes, which was stable for more than 15 days. This suspension of SWNTs in a quartz tube was kept at the center of the detection coil of the NMR spectrometer.

For dynamic measurements of confined water inside the SWNT, we have used the 500 MHz spectrometer. The diffusion measurements were carried out using a BRUKER QNP probe with the sample filled up to 1.5 cm in a 5 mm diameter standard NMR tube. The pulse sequence used in our experiment is stimulated echo pulsed field gradient (STEPFG) using bipolar gradients.[33,42] The basic mechanism of any PFG method is that a magnetic field gradient is applied across the volume of the sample by using a z-axis gradient coil. This field is in addition to the constant B_0 ($\hat{z}$) field of the NMR magnet. Thus, the resultant magnetic field varies along the z-direction as $B(z) = B_0 + gz$, where $g = (\partial B_z/\partial z)\hat{z}$ is the strength of the gradient field. The nuclear spins subject to this gradient field will precess with an angular frequency of $\omega(z) = -\gamma B(z)$, where γ is the gyromagnetic ratio, and consequently, the acquired phase will be $\phi(z) = -\gamma B(z)\delta$, where δ is the duration of applied gradient field. Now, if we apply a normal $\pi/2$ rectangular radio frequency pulse then the magnetization vector will be tilted in transverse direction and precess with a linearly varying phase describing a regular helix along the z-direction. In the absence of diffusion, this uniformly dephased magnetization can be almost (except the part lost due to T_2 relaxation) fully recovered as an echo by applying a π pulse after a time t. The π pulse reversed the phase, and the helical magnetization is refocused to a planar ribbon. However, diffusion of molecules randomizes the phase, which smears out the magnetization helix resulting in reduced magnitude of the

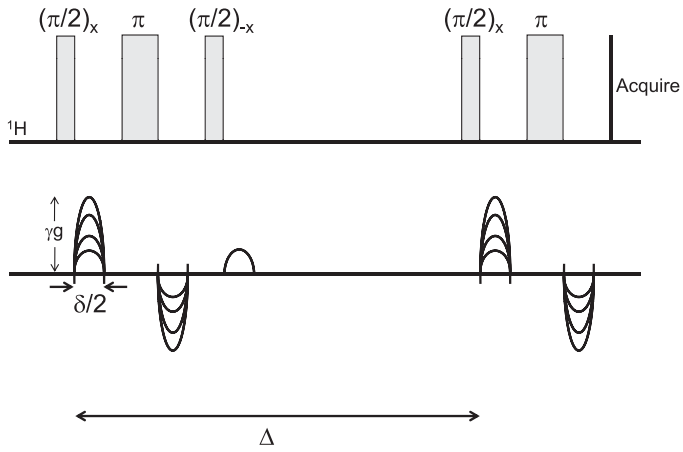

Figure 9. Standard stimulated echo pulse sequence incorporating bipolar gradient used in the experiment.

recovered magnetization. The attenuation of the signal is higher if the mean squared displacements ($\langle Z^2(t)\rangle$) of the molecules are more. The relation between the PFG NMR attenuated signal, I, to the MSD ($\langle Z^2(t)\rangle$) for an isotropic diffusion is described by eq 1,[33] and thus, MSD ($\langle Z^2(t)\rangle$) can be measured by varying the gradient field strength.

Figure 9 shows the pulse sequences for the STEPFG method.[43] The advantage of the STEPFG method is, in the case of slow diffusion, that the NMR signal will be attenuated more by T_2 relaxation than by diffusion. In such cases, it will be advantageous to flip the spins to the longitudinal direction, where the slower T_1 relaxation process dominates, and let water molecules diffuse while the magnetization is in the z-direction. Final measurement is done by flipping back the spins to the transverse direction and then applying the refocusing gradient and acquiring the signal. The polarity of the gradient field is reversed to diminish the eddy currents induced by the short gradient pulse. A spoiler gradient in Figure 1 between the second and the third $\pi/2$ pulse was used to dephase the unwanted magnetization. The proton $\pi/2$ pulse was a duration of 9.5 μs in our experiment. The parameters, δ (the duration of the gradient pulse) and Δ, which is related to the diffusion time, were optimized to produce minimal attenuation of the signal for 5% of the gradient strength and full attenuation for 95% of the gradient strength. In our experiments, 16 values of gradient fields varying from $g = 0$ to $g = 0.33$ Tm^{-1} were used. The δ value varied from 3 to 5 ms. The diffusion time, t, is related to Δ as $t = (\Delta - \delta/3)$; Δ is varied from 10 to 200 ms. Typically, 128 scans per experiment were used with a 5 s relaxation delay between scans. To reduce noise at higher attenuation, a uniform line broadening of 20 Hz was used. Low temperatures were maintained by using cooled nitrogen gas evaporated from the liquid nitrogen. Calibration of gradient strength was carried out using a standard Bruker sample of "doped water", which is 1% H_2O in D_2O with 0.1 g/L $GdCl_3$ at 25 °C.

Acknowledgment. We are grateful to Prof. C.N.R. Rao for the SWNT samples. A.K.S. thanks the Department of Science and Technology (DST) for financial assistance under the Nano-mission project. The use of the DST sponsored NMR facilities under the SAIF programme at NMR Research Centre is acknowledged.

REFERENCES AND NOTES

1. Zangi, R. Water Confined to a Slab Geometry: A Review of Recent Computer Simulation Studies. *J. Phys.: Condens. Matter* **2004**, *16*, S5371–S5388.
2. Saito, R.; Dresselhaus, G.; Dresselhaus, M. S. *Physical Properties of Carbon Nanotubes*; Imperical College Press: London, 1998.
3. Koga, K.; Gao, G. T.; Tanaka, H.; Zeng, X. C. Formation of Ordered Ice Nanotubes Inside Carbon Nanotubes. *Nature* **2001**, *412*, 802–805.
4. Hummer, G.; Rasaiah, J. C.; Noworyta, J. P. Water Conduction through the Hydrophobic Channel of a Carbon Nanotube. *Nature* **2001**, *414*, 188–190.
5. Koga, K.; Gao, G. T.; Tanakac, H.; Zeng, X. C. How Does Water Freeze Inside Carbon Nanotubes? *Physica A* **2002**, *314*, 462–469.
6. Martí, J.; Gordillo, M. C. Temperature Effects on the Static and Dynamic Properties of Liquid Water Inside Nanotubes. *Phys. Rev. E* **2001**, *64*, 021504-1–021504-6.
7. Gordillo, M. C.; Martí, J. Hydrogen Bond Structure of Liquid Water Confined in Nanotubes. *Chem. Phys. Lett.* **2000**, *329*, 341–345.
8. Striolo, A.; Chialvo, A. A.; Gubbins, K. E.; Cummings, P. T. Water in Carbon Nanotubes: Adsorption Isotherms and Thermodynamic Properties from Molecular Simulation. *J. Chem. Phys.* **2005**, *122*, 234712-1–234172-14.
9. Takaiwa, D.; Hatano, I.; Koga, K.; Tanaka, H. Phase Diagram of Water in Carbon Nanotubes. *Proc. Natl. Acad. Sci. U.S.A.* **2008**, *105*, 39–43.
10. Maniwa, Y.; Kataura, H.; Abe, M.; Suzuki, S.; Achiba, Y.; Kira, H.; Matsuda, K. Phase Transition in Confined Water Inside Carbon Nanotubes. *J. Phys. Soc. Jpn.* **2002**, *71*, 2863–2866.
11. Kolesnikov, A. I.; Zanotti, J.-M.; Loong, C.-K.; Thiyagarajan, P. A.; Moravsky, P.; Loutfy, R. O.; Burnham, C. J. Anomalously Soft Dynamics of Water in a Nanotube: A Revelation of Nanoscale Confinement. *Phys. Rev. Lett.* **2004**, *93*, 035503-1–035503-4.
12. Ghosh, S.; Ramanathan, K. V.; Sood, A. K. Water at Nanoscale Confined in Single-Walled Carbon Nanotubes Studied by NMR. *Europhys. Lett.* **2004**, *65*, 678–684.
13. Mao, S.; Kleinhammes, A.; Wu, Y. NMR Study of Water Adsorption in Single-Walled Carbon Nanotubes. *Chem. Phys. Lett.* **2006**, *421*, 513–517.
14. Sekhaneh, W.; Kotecha, M.; Weglikowska, U. D.; Veeman, W. S. High Resolution NMR of Water Absorbed in Single-Wall Carbon Nanotubes. *Chem. Phys. Lett.* **2006**, *428*, 143–147.
15. Matsuda, K.; Hibi, T.; Kadowaki, H.; Kataura, H.; Maniwa, Y. Water Dynamics Inside Single-Wall Carbon Nanotubes: NMR Observations. *Phys. Rev. B* **2006**, *74*, 073415-1–073415-4.
16. Fedders, P. A. Two-Point Correlation Functions for a Distinguishable Particle Hopping on a Uniform One-Dimensional Chain. *Phys. Rev. B* **1978**, *17*, 40–46.
17. Karger, J. Straightforward Derivation of the Long-Time Limit of the Mean-Square Displacement in One-Dimensional Diffusion. *Phys. Rev. A* **1992**, *45*, 4173–4174.
18. Karger, J. Long-Time Limit of the Self-Correlation-Function of One-Dimensional Diffusion. *Phys. Rev. E* **1993**, *47*, 1427–1428.
19. Hodgkin, A. L.; Keynes, R. D. The Potassium Permeability of a Giant Nerve Fibre. *J. Physiol.* **1955**, *128*, 61–88.
20. Riekert, L. Sorption, Diffusion, and Catalytic Reaction in Zeolites. *Adv. Catal.* **1970**, *21*, 281–322.
21. Levitt, D. G. Dynamics of a Single-File Pore: Non-Fickian Behavior. *Phys. Rev. A* **1973**, *8*, 3050–3054.
22. Kukla, V.; Kornatowski, J.; Demuth, D.; Girnus, I.; Pfeifer, H.; Rees, L. V. C.; Schunk, S.; Unger, K. K.; Karger, J. NMR Studies of Single-File Diffusion in Unidimensional Channel Zeolites. *Science* **1996**, *272*, 702–704.
23. Neher, E. Ion Channels for Communication between and within Cells. *Science* **1992**, *256*, 498–502.
24. Sakmann, B. Elementary Steps in Synaptic Transmission Revealed by Currents through Single Ion Channels. *Science* **1992**, *256*, 503–512.
25. Chen, D. P.; Eisenberg, R. S. Flux, Coupling, and Selectivity in Ionic Channels of One Conformation. *Biophys. J.* **1993**, *65*, 727–746.
26. Tajkhorshid, E.; Nollert, P.; Jensen, M. O.; Miercke, L. J. W.; O'Connell, J.; Stroud, R. M.; Schulten, K. Control of the Selectivity of the Aquaporin Water Channel Family by Global Orientational Tuning. *Science* **2002**, *296*, 525–530.

27. Lei, G.-D.; Sachtler, W. M. H. H/D Exchange of Cyclopentane on Pt/Mordenites: Probing for Monoatomic Pt Sites. *J. Catal.* **1993**, *140*, 601–611.
28. Nivarthi, S. S.; McCormick, A. V.; Davis, H. T. Diffusion Anisotropy in Molecular Sieves: A Fourier Transform PFG NMR Study of Methane in $AlPO_4$-5. *Chem. Phys. Lett.* **1994**, *229*, 297–301.
29. Gupta, V.; Nivarthi, S. S.; McCormick, A. V.; Davis, H. T. Evidence for Single File Diffusion of Ethane in the Molecular Sieve $AlPO_4$-5. *Chem. Phys. Lett.* **1995**, *247*, 596–600.
30. Hahn, K.; Kärger, J.; Kukla, V. Single-File Diffusion Observation. *Phys. Rev. Lett.* **1996**, *76*, 2762–2765.
31. Striolo, A. The Mechanism of Water Diffusion in Narrow Carbon Nanotubes. *Nano Lett.* **2006**, *6*, 633–639.
32. Mukherjee, B.; Maiti, P. K.; Dasgupta, C.; Sood, A. K. Strong Correlations and Fickian Water Diffusion in Narrow Carbon Nanotubes. *J. Chem. Phys.* **2007**, *126*, 124704-1–124704-8.
33. Callaghan, P. T. *Principles of Nuclear Magnetic Resonance Microscopy*; Clarendon: Oxford, 1991.
34. Callaghan, P. T. Pulsed Field Gradient Nuclear Magnetic Resonance as a Probe of Liquid State Molecular Organization. *Aust. J. Phys.* **1984**, *37*, 359–387.
35. Stejskal, E. O.; Tanner, J. E. Spin Diffusion Measurements: Spin Echoes in the Presence of a Time-Dependent Field Gradient. *J. Chem. Phys.* **1965**, *42*, 288–292.
36. Zhao, J.; Buldum, A.; Han, J.; Lu, J. P. Gas Molecule Adsorption in Carbon Nanotubes and Nanotube Bundles. *Nanotechnology* **2002**, *13*, 195–200.
37. Werder, T.; Walther, J. H.; Koumoutsakos, P. Hydrodynamics of Carbon Nanotubes—Contact Angle and Hydrophobic Hydration. Technical Proceedings of the Second International Conference on Computational Nanoscience and Nanotechnology-ICCN 2002; Vol. 2, pp 490−493.
38. Walther, J. H.; Jaffe, R.; Halicioglu, T; Koumoutsakos, P. Carbon Nanotubes in Water: Structural Characteristics and Energetics. *J. Phys. Chem. B* **2001**, *105*, 9980–9987.
39. Bekyarova, E.; Hanzawa, Y.; Kaneko, K.; Albero, J. S.; Escribano, A. S.; Reinoso, F. R.; Kasuya, D.; Yudasaka, M; Iijima, S. Cluster-Mediated Filling of Water Vapor in Intratube and Interstitial Nanospaces of Single-Wall Carbon Nanohorns. *Chem. Phys. Lett.* **2002**, *366*, 463–468.
40. Ligget, T. *Interacting Particle Systems*; Springer-Verlag: New York, 1985.
41. Vivekchand, S. R. C.; Jayakanth, R.; Govindaraj, A.; Rao, C. N. R. The Problem of Purifying Single-Walled Carbon Nanotubes. *Small* **2005**, *1*, 920–923.
42. Johnson, C. S. Diffusion Ordered Nuclear Magnetic Resonance Spectroscopy: Principles and Applications. *Prog. NMR Spectrosc.* **1999**, *34*, 203–256.
43. Cotts, R. M.; Hoch, M. J. R.; Sun, T.; Markert, J. T. Pulsed Field Gradient Stimulated Echo Methods for Improved NMR Diffusion Measurements in Heterogeneous Systems. *J. Magn. Reson.* **1989**, *83*, 252–266.